NJC

Accepted Manuscript

ROYAL SOCIETY OF CHEMISTRY

www.rsc.org/njc

Probing the self-aggregation behavior and counter ion distribution of a copper surfactant complex

Ravneet Kaur[a], Sakshi Gupta[a], Surinder K. Mehta[a,*], Yosuke Imai[b], Takanori Takiue[b], Hiroki Matsubara[b], Makoto Aratono[b*]

[a]*Department of Chemistry & Centre of Advanced Studies in Chemistry, Panjab University, Chandigarh – 160 014, India*

[b]*Department of Chemistry, Faculty of Sciences, Kyushu University, Hakozaki 6-10-1, Higashiku, Fukuoka 812-8581, Japan*

*Corresponding authors:

Tel.: +91-172 2534423, Fax: +91-172-2545074, *E-mail*: skmehta@pu.ac.in (S.K.M.);

Fax: +81 92 642 2607, *E-mail*: aratono@chem.kyushu-univ.jp (M.A.)

Abstract:

In the present work, a new copper surfactant complex $[Cu(BrCl_2)(C_{12}H_{25}N(CH_3)_3)]$ was synthesized and characterized. Its organization at the air-water interface and in bulk aqueous medium was investigated. The aggregation behavior and adsorption pattern of the metallosurfactant revealed important information about the molecular organization and counter ion distribution which is hitherto unknown. The critical micellization concentration and optical thickness of the copper surfactant was determined using surface tension, cyclic voltammetry and ellipsometry techniques, respectively. The X-ray absorption fine structure technique was applied to the copper surfactant solution under both total reflection (TRXAFS) and transmission conditions to understand the ion organization at the interface and in the bulk, respectively. The Br and Cu K-edge absorption revealed the presence of Br^- ion but the absence of Cu^{2+} ion at the interface and in the inner core of micelles. Furthermore, Br^- ion was found to exist in two solvation states, assigned as "free-Br" and "bound-Br". Even the surface excess concentration of the ions was precisely determined from the adsorbed film of copper surfactant using external reflection absorption (ERA)-FTIR spectroscopy.

Keywords: Metallosurfactant, Copper cation, Total reflection XAFS, Counter ion distribution, Aggregation behavior

1. Introduction

The origin of surfactants or amphiphiles dates back to 1500 BC when the first types of soaps were produced. Since then, the surfactant chemistry has been growing in leaps and bounds providing exciting possibilities to researchers from both experimental and application point of view. Metallosurfactants or metal surfactant complexes have been a recent addition to the vast field of surfactant chemistry. These metalloamphiphiles possess characteristic features of surfactants such as emulsification, repellency, self aggregation, micellization and metals such as redox activity which show promising applications in a number of industries dealing with detergents[1], drug delivery[2,3], enhanced oil recovery[4], solubilization of insoluble compounds[5], catalysis[6,7], nanoparticles[8] etc. Taking into account the relevance and utility of new surfactants, it becomes exceedingly important to study their aggregation behavior and physico-chemical properties.

A lot of research papers have contributed towards developing an understanding of the surfactant chemistry at the surface and interfaces. The surfactant adsorption at the hydrophilic solid –liquid interface is a very complex yet interesting phenomenon. The factors affecting surfactant adsorption and its experimental studies have been excellently reviewed in detail by Paria and Khilar[9]. While a number of studies are available in literature investigating the micellization of conventional surfactants and their molecular interactions[10], however, the metallosurfactant chemistry has not been explored much with respect to their aggregation behavior. Metallosurfactants illustrate fundamental surfactant-like properties as well as some interesting non-classical behavior. In case of conventional surfactants, the counter ions, hydrophobic alkyl chains and head groups influence the surface density, critical micelle concentration (cmc) and even the amphiphilic assemblies formed[11-14]. The incorporation of a metal ion in the head group or in the counter ion species of the surfactant is bound to affect their aggregation behavior. However, a systematic study towards metallosurfactant adsorption and monomer organization has not been dealt with so far, although they have been used in quite a number of applications especially those involving catalysis[15-17].

Micellar systems incorporating transition metal complexes have been used for carrying out organic synthesis in water. In a report by Yagyu et al.[17], palladium (Pd) complexes acted as efficient catalysts for Heck and Suzuki reactions proceeding through a Pd (II) to Pd (0) redox reaction. It has been observed that the key point controlling the formation of a catalytically active metallomicelle in aqueous media is the location of metal ion i.e. the metal ion should not stay in the core of the micelle but at the periphery to facilitate facile transfer of reactant and product moieties for an effective catalytic cycle. Therefore, the metallosurfactant should be designed in such a way that the metal is stabilized at the surface of micelle away from its inner cavity. Thus, it becomes exceedingly important to determine the location and organization of metal ions and counter ions before applying metallosurfactants to catalysis.

There have been a few reports in a literature focusing on the organization of metal ions in monolayers and interfaces e.g. Jayathilake et al.[18] studied the molecular organization in the monolayers of ligand surfactant and its copper-containing complexes using vibrational SFG spectroscopy. Double-tailed metal-ligand surfactants resulting from chelation of copper (II) by two ligand surfactants also formed well-aligned monolayers; however, the degree of packing and conformational order was not as high as that for a single-tailed metal-ligand surfactant because of its bulky head group. In a report by Nagatani et al.[19] EXAFS analysis for the copper (II) complexes i.e. copper (II) porphyrins (CuPP) and copper (II) chlorophyllin (CuChl) at the air–water interface was achieved for the first time at a monolayer level by using the polarized TR-XAFS technique in the fluorescence mode. The local coordination structures of CuPP and CuChl were characterized in the respective polarization plane. However, in another study the inorganic ions and electrolytes showed negative adsorption at the air-water interface[20]. However, the organization of metallosurfactant monomers at the interface and surface still remains unclear.

The main objective of the present work is to investigate the aggregation and adsorption behavior of the metallosurfactant i.e. copper surfactant complex $[Cu(BrCl_2)(C_{12}H_{25}N(CH_3)_3)]$. The focus is to explore the molecular organization and counter ion distribution of the metallosurfactant at the air-water interface and in the bulk which is hitherto unknown. This information is highly valuable to further employ metallosurfactants in redox or catalysis based applications and also for nanoparticle fabrication. To this end we use total-reflection X-ray absorption fine structure (TRXAFS), surface tension, ellipsometry, external reflection absorption (ERA)-FTIR spectroscopy and cyclic voltammetry to obtain mesoscopic information about the metallo-aggregation behavior. We demonstrate that the surface excess concentration of various species, the mean optical thickness of the monolayer at the interface and the organization of ions at the interface as well as bulk can be precisely determined, which can be very useful for further applications.

2. Experimental

2.1. Materials and Methods

Copper (II) chloride and dodecyltrimethyl ammonium bromide (DTAB) having purity>98% were purchased from Sigma-Aldrich. The materials were used as received. Deionised doubly distilled water (using Labpure Analytica Bioage instrument and further distilled using $KMnO_4$) was used for conducting experiments. FTIR (Fourier Transform Infra Red) measurements were performed on a Perkin Elmer (RX1) FTIR spectrophotometer. For ^1H-NMR spectra, Bruker Avance 300 spectrometer (300 MHz) was used with $CDCl_3$ as the solvent. For electrochemical studies, cyclic voltammeter Autolab Type III electrochemical system, equipped with GPES software from Metrohm was used with Platinum wire as counter electrode, Platinum electrode as working electrode and Ag/AgCl as reference electrode was used. Surface tension was measured on a K20 Krüss tensiometer (Germany) with an error limit of ±0.1 mNm^{-1} using the Ring Method at 298.15 K. ERA-FTIR spectra were collected with a Perkin-Elmer FTIR spectrometer (Spectrum One), equipped with an external reflection module (Specac). The detection area was about 1 cm^2. The mercury-cadmium-telluride (MCT) detector was used by cooling it with liquid nitrogen. The measurements were recorded in situ at the air-water surface. The solution was first introduced into the measuring cell (w x d x l = 3.6 cm x 0.9 cm x 5.0 cm), and subsequently, FTIR light was applied to the surface. TR-XAFS experiment was performed by using the synchrotron radiation at BL-7C of the Photon Factory in the National Laboratory for High Energy Physics (Tsukuba, Japan). Energy of X-ray was scanned to cover the Br–K edge and Cu edge from 13391 to 13663 eV and 8850 to 9500 eV, respectively. X-ray beam was monochromatized by a double-crystal Si (111) monochromator and then tilted to make incident angle of the X-ray, 1 mrad so as to satisfy the total reflection condition at the solution surface. The gas-ionization chamber placed in front of the solution cell counts the incident beam intensity, I_0, by using N_2 gas. The solution cell itself was filled with He gas flowing at a constant rate. The electrode equipped with the cell wall collects helium ions generated by Auger electrons from bromide ions at the surface. Then the signal intensity, I, was detected by the total conversion He^+ ion-yield method. The solution temperature was kept constant at 298.15 K by circulating thermostated water. The XAFS spectrum was obtained by plotting I/I_0 against X-ray energy[21-24]. The phase modulated ellipsometer used to determine the optical thickness was computer controlled and custom built. It possessed a Beaglehole Instruments (Wellington, New Zealand) birefringence modulator, which modulated the phase of a 5 mW HeNe laser beam at

50 kHz.

2.2. Synthesis of copper surfactant complex

Copper surfactant complex with the formula $[Cu(BrCl_2)(C_{12}H_{25}N(CH_3)_3)]$ was synthesized by refluxing equimolar quantities of copper chloride and dodecyl trimethylammonium bromide (DTAB) in ethanol for three hours. Immediate color change was observed from blue to brown on the addition of ethanol. The obtained residue after refluxing and rotary evaporation was recrystallized using dichloromethane-ethyl acetate mixture. The synthesized metallosurfactant has been used for further characterization and experiments.

3. Results and Discussion

The synthesized copper surfactant has been characterized using various spectroscopic techniques. Furthermore, the self aggregation behavior of the synthesized surfactant has been analyzed completely using various complementary techniques such as surface tension, cyclic voltammetry, ERA-FTIR Spectroscopy, ellipsometry and TRXAFS.

3.1. Spectroscopic Characterization

The copper surfactant has been characterised using Fourier transform infra red (FTIR) spectroscopy and ^{1}H nuclear magnetic resonance (NMR) spectroscopy

3.1.1. FTIR Spectroscopy**:** The FTIR spectra of the reactant DTAB and the copper complexed DTAB depicted the presence of almost similar bands. However, the copper complexed DTAB showed some extra peaks in addition to those of pure DTAB corresponding to metal halide bonding. The bands present in the region below 750 cm^{-1} can be attributed to metal complexation, where the peaks observed at 430 cm^{-1} and 550 cm^{-1} are due to Cu-Cl and Cu-Br bond formation, respectively, pointing towards metal complexation with ligands[25] (Figure 1). The sharp peaks observed at 2929 cm^{-1} and 2851 cm^{-1} correspond to CH_2 asymmetric and symmetric stretching, respectively. The peak at 1469 cm^{-1} corresponds to the vibrations of methylene (CH_2) group while the one at 970 cm^{-1} can be attributed to C-N vibrations.

3.1.2. ^{1}H-NMR Spectroscopy**:** ^{1}H NMR spectra for free and copper complexed DTAB are quite similar, except for the fact that the spectrum of DTAB is better resolved due to absence of interference from the paramagnetic character of copper. Upon complexation with the metal ions, all the proton signals of the ligand undergo chemical shift as summarized in Table 1. But maximum shift is observed in the proton signals of methyl present in $-N(CH_3)_3$ group.

The larger shift of this signal is consistent with the ionic bonding between quaternary ammonium ion and bromide ion. This signal shows maximum downfield shift after complexation with metal because bromide gets coordinated to copper cation, which affects the bonding with the quaternary ammonium group.

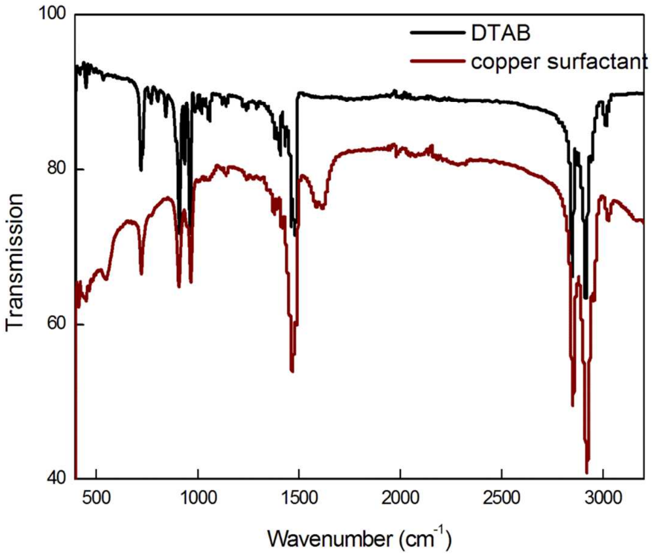

Fig. 1 FTIR spectra for DTAB and copper surfactant complex.

Table 1 ^{1}H-NMR shifts for DTAB and copper surfactant complex.

^{1}H-NMR signal	DTAB (ppm)	Copper surfactant complex (ppm)
CH_3-CH_2-	0.866	0.875
$CH_3-(CH_2)_9-CH_2-CH_2-N^+$	1.244	1.305
$CH_3-(CH_2)_9-CH_2-CH_2-N^+$	1.646	1.679
$CH_3-(CH_2)_9-CH_2-CH_2-N^+$	1.730	2.017
$CH_3-(CH_2)_9-CH_2-CH_2-N(CH_3)_3^+$	3.540	4.857

3.2. Self aggregation behavior

3.2.1. Determination of critical micelle concentration (cmc): cmc of the copper surfactant has been determined using techniques such as surface tension and cyclic voltammetry taking into account the amphiphilic and redox behaviour of the surfactant synthesized.

Surface tension (γ) has been measured as a function of surfactant concentration at 298.15 K. Figure 2 shows the surface tension curve of copper surfactant complex indicating the arrangement of monomers in different states, with change in concentration giving the cmc value. The surfactant monomers exist in a gaseous state at very low concentrations (~ 0.5 mM). However, on moving to higher concentrations (until cmc ≈ 9.5 mM) an expanded state is adopted whereas above cmc, the surfactant monomers arrange to form micelles. In fact, it is difficult to completely purify the synthesized copper surfactant used. This is reflected in the measured surface tension values which are a little scattered especially in the low concentration region. Therefore, it was decided to use only the data around cmc to estimate the maximum surface adsorption here. The slope of γ *vs.* log concentration (conc.) curve gives an idea about the maximum surface excess concentration (Γ_{max}) i.e. the amount of adsorbed surfactant at the interface which can be calculated using the Gibbs adsorption equation

$$\Gamma_{max} = \frac{1}{nRT} \frac{\partial\gamma}{\partial \ln C}_{cmc}$$

where n=1, for nonionic surfactant (1)
n=2, for ionic surfactant

where R is the gas constant and T is the absolute temperature. It is a measure of the effectiveness of the surfactant adsorption at the interface, since, it is the maximum value which adsorption can attain[11].

Our thermodynamic formulation for surface adsorption for ionic surfactant with added electrolyte clarified that $\Gamma = -(1/RT)(\partial\gamma/\partial \ln C)$ expresses the sum of surface density of each chemical species[26] and the validity of estimating the surface adsorption of ionic species using this equation was verified by using TRXAFS technique in our previous study[27,28]. For the copper surfactant used in this study, $= \Gamma_{\mathrm{DTA}} + \Gamma_{\mathrm{Cu}} + \Gamma_{\mathrm{Br}} + \Gamma_{\mathrm{Cl}}$, therefore, Γ_{DTA} could not be simply obtained by using eq. (1) and $n = 2$ as is the case with pure DTAB surfactant. Actually in this case, the surface density of each species cannot be determined only by thermodynamic analysis. Therefore, ERA-FTIR technique has been used to determine Γ_{DTA} as discussed later. The cmc value obtained for the copper surfactant complex (9.5 mM) is smaller than the precursor cationic surfactant DTAB (15.2 mM (surface tension) [29], 15 mM (surface tension)[30]) indicating a higher tendency for self-aggregation on introduction of the copper ion to the pure DTAB surfactant.

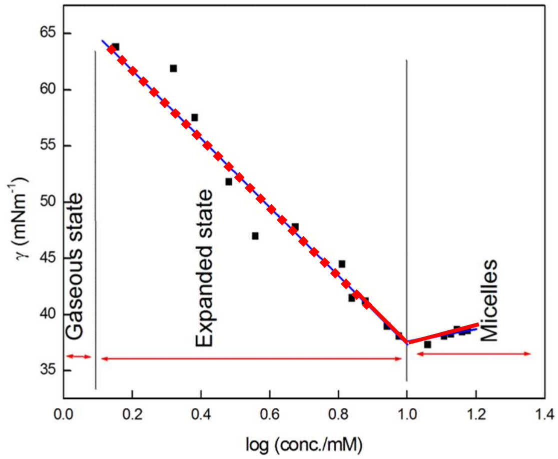

Fig. 2 Surface tension curve for copper surfactant complex.

Cyclic voltammetry was further used to determine the cmc value of the copper surfactant complex. The calculation of cmc by plotting i_p *vs.* conc. using cyclic voltammetry has already been carried out long back by Mandal et al.[31] for commercially available surfactants such as SDS, Triton-X 100, Tween-80. However, we use this approach to ascertain the cmc value of the copper surfactant complex as depicted in Fig. 3 (The cyclic voltammogram and redox potential of the complex have been provided in supplementary information). For electrochemical studies, Platinum wire was used as counter electrode, Platinum electrode as working electrode and Ag/AgCl as reference electrode in the presence of sodium chloride (1 mM) as electrolyte. However, no probe was used to determine the cyclic voltammograms as the copper surfactant itself is capable of showing redox active behavior. The cmc value determined was 7.8 mM, lower than that obtained from surface tension (9.5 mM) technique which may be attributed to the difference in temperature (Surface tension studies were carried out by maintaining the temperature at 25 ^{o}C but cyclic voltammetry was carried out at room temperature) and partially to the presence of additional electrolyte as well.

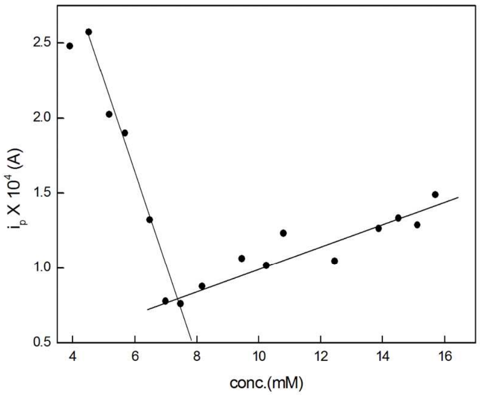

Fig. 3 i_p *vs.* conc. plot to determine cmc of copper surfactant complex.

3.2.2. Surface density analysis of the adsorbed surfactant: To have an idea about the structural behavior of the surface films, ERA-FTIR spectroscopy was utilized. The surface density of the surfactant adsorbed in the surface film is reflected from the peak height of the FTIR spectrum which is a measure of the total amount of CH_2 groups adsorbed while the wavenumber gives information on the conformational state of the film i.e.; condensed films are characterized by a vibration at 2918 cm^{-1} due to antisymmetric CH_2 stretching, while expanded films are characterized by a vibration at 2925 cm^{-1}. The spectra were recorded at different concentrations for copper surfactant complex ranging from 3-19 mM (Fig. 4). Two bands are clearly observed at around 2920 cm^{-1} and 2850 cm^{-1} owing to antisymmetric and symmetric CH_2 stretching, respectively. The estimated wavenumber and peak height values plotted in Figure 5 shows that the stretching values of CH_2 group shift to lower ones as the concentration of surfactant increases. The wavenumber values decrease very sharply till cmc from 2923.7 to 2921 cm^{-1} and then become somewhat constant. The frequencies of CH_2 stretching vibration bands are very sensitive to any type of conformational changes occurring in the hydrocarbon chain. The shifting to lower values suggests a transition going from disorder to order i.e. the hydrocarbon chains become more ordered and show closer packing with increasing concentration[32]. The wavenumber values as depicted in Fig. 5 point towards the presence of an expanded phase. Judging from the values of peak height and wavenumber, it can be inferred that the adsorbed film adopts an expanded conformation.

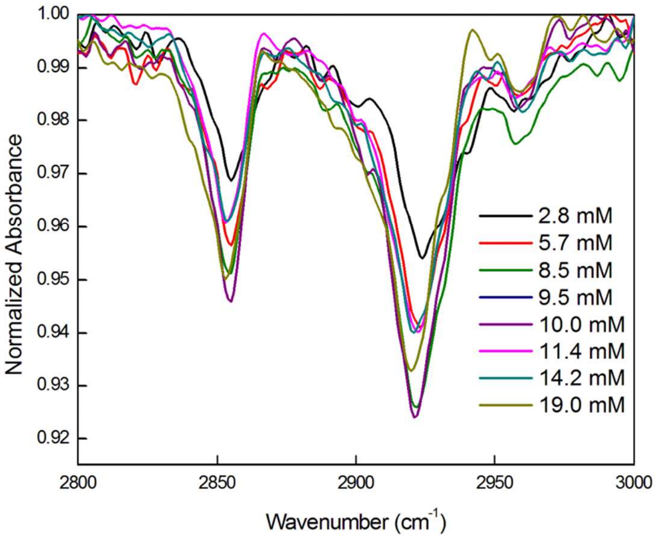

Fig. 4 ERA-FTIR spectra for copper surfactant at different molar concentrations of copper surfactant complex.

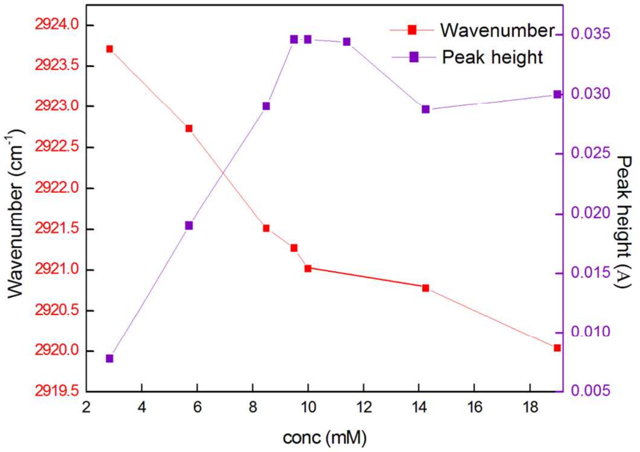

Fig. 5 Concentration dependence of peak height and wavenumber of CH_2 asymmetric stretching peaks observed in ERA-FTIR spectra of copper surfactant complex.

The surface density of DTA ion as calculated from ERA-FTIR spectroscopy, $\mathit{\Gamma}_{\mathrm{DTA}}$= 3.71 μ mol m^{-2} is larger than $\mathit{\Gamma}_{\mathrm{DTA}}$ for DTAB surfactant (3.42 μ mol m^{-2} using surface tension)[30]. This result supports the idea that in the aqueous solution Cu^{2+} and Cl^{-} ions exist as electrolyte for DTAB as the surface density of DTA ion is increased due to the shielding effect because of the repulsion between DTA ions.

3.2.3. Determination of film thickness: Ellipsometry is a classical method of determining film thickness or thickness of the layer formed at the interface which was used to measure optical thickness. The thickness of a surfactant layer depends upon the size of hydrophobic alkyl chain, head group, counter ion and roughness of the sample. In the present case, ellipsometric studies were carried out at two different concentrations; (a) very dilute surfactant concentration i.e. 0.05 mM to calculate the value of ellipticity, which can solely be attributed to roughness, (b) higher surfactant concentration of 5 mM, which takes into account the effect of the size of alkyl chain, head group and counter ion. The coefficient of ellipticity, $\bar{\boldsymbol{\rho}}$ is reasonably approximated to be the sum of roughness, $\bar{\boldsymbol{\rho}}_{\boldsymbol{r}}$ and three other contributions from the hydrophilic groups, $\bar{\boldsymbol{\rho}}_{\boldsymbol{h}}$ counter ions, $\bar{\boldsymbol{\rho}}_{\boldsymbol{i}}$ and hydrocarbon chains $\bar{\boldsymbol{\rho}}_{\boldsymbol{c}}$, which can be expressed by the equation,

$$\bar{\rho} = \bar{\rho}_r + \bar{\rho}_i + \bar{\rho}_h + \bar{\rho}_c \qquad (2)$$

The value of $\bar{\rho}$ as obtained from ellipsometry experiment is but -2.30581 x 10^{-3} the aim of the experiment here is to estimate the thickness of hydrocarbon layer d_c in the terms of $\bar{\rho}_c$. Therefore, the values of $\bar{\rho}_r$, $\bar{\rho}_i$ and $\bar{\rho}_h$ have to be determined with reasonable assumptions as explained previously in literature[33]. The calculations used have been discussed below briefly.

(a) *Roughness* $\overline{(\rho_r)}$

$\bar{\rho}_r = 0.495 \times 10^{-3}$ calculated using eq. (3):

$$\overline{\rho}_r = 0.4 \times 10^{-3}\sqrt{\frac{72}{\gamma}} \tag{3}$$

where γ = 47 mN m^{-1} at 5 mM.

(b) *Hydrophilic group and counter ion Layers* $(\bar{\rho}_h, \bar{\rho}_i)$

All layers in this system are assumed to be isotropic, and eq. (4) given below is used to determine $\bar{\rho}_j$ values for all layers.

$$\bar{\rho}_j = \frac{\pi\sqrt{\varepsilon_a + \varepsilon_w}}{\lambda(\varepsilon_a - \varepsilon_w)}\frac{(\varepsilon_j - \varepsilon_a)(\varepsilon_j - \varepsilon_w)}{\varepsilon_j} d_j \ (j = h, i) \tag{4}$$

where values of λ, ε_a and ε_w are known to be 632.9 nm, 1, and 1.776, respectively, while ε_j and d_j have to be estimated.

- Determination of $\boldsymbol{\bar{\rho}_h}$

This layer is assumed to be composed of trimethyl ammonium (TMA) head groups and water molecules. To calculate $\bar{\rho}_h$ using eq. (4) given above, the d_h value used is 8 Å from a previous study[33] and ε_h value is estimated using Lorentz-Lorenz effective medium approximation, eq. (5), as given below

$$\frac{\varepsilon_h - 1}{\varepsilon_h + 2} = \left(\frac{\varepsilon(\mathrm{TMA}) - 1}{\varepsilon(\mathrm{TMA}) + 2}\right)\phi(\mathrm{TMA}) + \left(\frac{\varepsilon_w - 1}{\varepsilon_w + 2}\right)\left(1 - \phi(\mathrm{TMA})\right) \tag{5}$$

where $\phi(\mathrm{TMA})$ is the volume fraction of TMA which comes out to be 0.14446 (Detailed calculations can be found in Supplementary Information). Substituting, $\phi(\mathrm{TMA})$ and $\varepsilon(\mathrm{TMA}) = 2.38$ [33] in eq. (5), the value of ε_h is estimated as 1.853. Substituting above values in eq. (4), value of $\bar{\rho}_h$ is found to be -0.3022×10^{-3}.

- Determination of $\boldsymbol{\bar{\rho}_i}$

This layer is considered to be composed of Cl$^-$, Br$^-$ and water molecules. $\bar{\rho}_i$ is again calculated using eq. (4), assuming d_i to be equal to Debye length, $r_D = 2.2975 \times 10^{-9}$ m (Detailed calculations in Supplementary Information). Just as in the case of TMA, the volume fraction of Br$^-$ and Cl$^-$ is calculated; $\phi(\mathrm{Br}) = 8.5179 \times 10^{-3}$, $\phi(\mathrm{Cl}) = 1.4363 \times 10^{-3}$. Substituting d_i, $\phi(\mathrm{Br})$ and $\phi(\mathrm{Cl})$, in eq. (5) ε_i is calculated which finally leads to the value of $\bar{\rho}_i$ ($\bar{\rho}_i = -0.23074 \times 10^{-3}$).

Therefore, substituting the values of $\bar{\rho}_i$, $\bar{\rho}_h$,$\overline{\rho}_r$, $\bar{\rho}$ in eq. (2) the value of $\bar{\rho}_c$ is calculated to be -2.267906×10^{-3} which leads to the thickness of hydrocarbon layer d_c using eq. (4) where, $\varepsilon_c = 2.02$ (The value for dodecane as given in reference number 33). The value of d_c or optical thickness comes out to be 1.09 nm. This is observed to be shorter than the length of a dodecyl hydrocarbon chain in all trans conformation and fully stretched state. This value implies that the adsorbed film exists in expanded state and not condensed one.

3.2.4. Surface concentration and solvation structure studies of surfactant: The XAFS under the total reflection condition (TRXAFS) was applied to the adsorbed films at the air-water interface to obtain; (a) the surface concentrations or surface distribution of the ions from the K-edge absorption intensity, (b) solvation structure of surface adsorbed ions from the XAFS analysis. TRXAFS was applied to obtain information on the solvation structure of Br^- ions in the adsorbed film of copper surfactant complex. The signal intensity *vs.* photon energy *E* curves have been displayed for aqueous solutions of copper chloride (200 mM) as blank and copper surfactant solution just below the cmc value at 9.5 mM in Fig. 6. The penetration depth of incident X-ray is experimentally estimated to be about 10 nm[34] and in this surface region of copper chloride ($CuCl_2$) aqueous solution, it could be estimated that about 2 $\boldsymbol{\mu\,\mathrm{mol\,m^{-2}}}$ of Cu^{2+} ions exist $[\mathbf{200(mM)} \times \mathbf{10(nm)} = \mathbf{0.2} \times \mathbf{10^{3}(mol\,m^{-3})} \times \mathbf{10} \times \mathbf{10^{-9}(m)} = \mathbf{2} \times \mathbf{10^{-6}(mol\,m^{-2})}]$. The jump at around 9000 eV in the copper chloride $CuCl_2$ solution is the K-edge absorption due to those copper ions present at the air-water interface. This peak is absent in case of copper surfactant complex which reveals that none of the copper ions are present in the range of detection depth at the air-water interface. TRXAFS was further applied to get the concentration of Br^- ions at the interface and transmission XAFS to get information about the bulk behavior of Br^- ions.

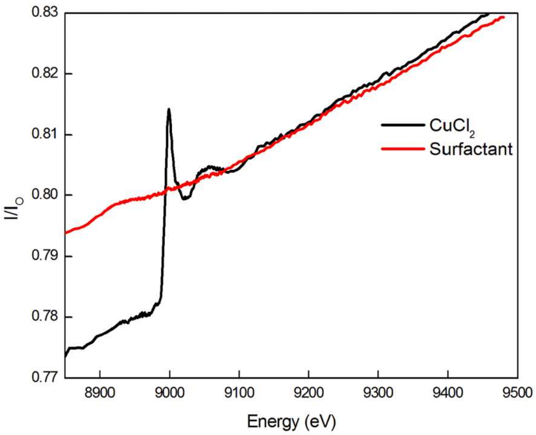

Fig. 6 K-edge X-ray absorption spectra of copper ions for aqueous solutions of $CuCl_2$ and copper surfactant complex.

TRXAFS gives an idea about the state of Br$^-$ ion, whether they are bound or free. In free Br state, Br$^-$ ions are assumed to be fully hydrated and in bound Br state, Br$^-$ ions are partially dehydrated and adsorbed to the hydrophilic groups of surfactant ions at the surface[35]. It was observed that all of Br$^-$ ions exist in bound state at the air-water interface (Fig. 7 (b)). Therefore, it can be inferred that the hydrophobic chain and Br$^-$ occupy the interface with the negatively charged Br$^-$ ion forming a kind of ion pair association. Transmission XAFS revealed that the χ spectra changed with the molarity. Br$^-$ ions were present in a free state initially and with increase in molarity, move to bound state. Hence, Br$^-$ ions can be present in either bound or free state, i.e. at 9 mM concentration all the surface Br$^-$ ions were present in the six hydrated bound-Br state but at 50 mM concentration a fraction of Br$^-$ was present in bound state and rest were free as shown in Fig. 7 (a). The fraction of free Br$^-$ ions at 50 mM can be estimated by using the relation given below.

$$\chi_{50\,\mathrm{mM}} = \alpha_{\mathrm{free}}\chi_{\mathrm{free}} + \alpha_{\mathrm{bound}}\chi_{\mathrm{bound}} \qquad (6)$$

$\chi_{50\,\mathrm{mM}}$, χ_{free} and χ_{bound} express EXAFS spectra for the sample, free-Br and bound-Br, respectively, while α_{free} and α_{bound} are the fractions of free-Br and bound-Br, respectively.

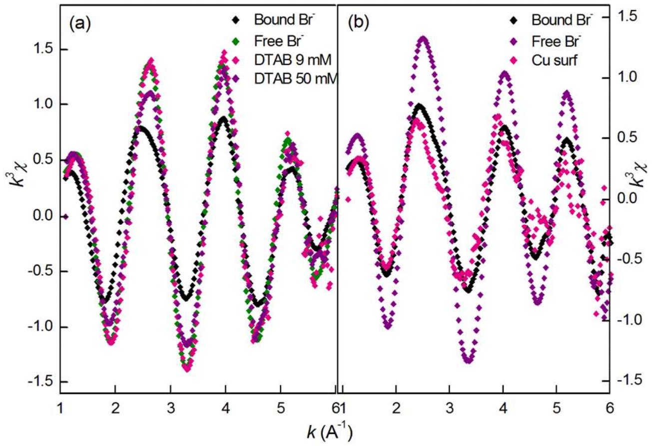

Fig. 7 EXAFS k$^3\chi$ spectra of Br$^-$ ions of the copper surfactant complex using (a) Transmission (b) Total reflection XAFS.

The estimated value for α_{bound} at 50 mM is about 0.36 and α_{free} is 0.64, which implies that 36% of Br$^-$ ion is in bound state and 64% of Br$^-$ ion is in the free state at 50 mM concentration. It is observed that α_{bound} for micelle at 50 mM is much smaller than α_{bound} for adsorbed film at 9.5 mM (almost unity). Taking into account the fact that in spherical micelle each headgroup is relatively loosely packed in wedge like spaces and thus, requires lesser electrostatic shielding as compared to the planar interface (showing greater ion association with bromide ions), it can be inferred that the shape of the interface (spherical or planar) could influence the distribution of counterions as well. Therefore, it is possible that the negative adsorption of Cu^{2+} due to electrostatic repulsion is greater at the surface of micelle where larger amount of positive charges are present as compared to the surface adsorbed film. Similar result [36] was obtained while exploring inorganic salt–dodecylammonium chloride mixtures. The dodecylammonium ion (DA^+) expelled inorganic cation from both the adsorbed film and the surface of micelle, and negative adsorption of metal ions in these systems was greater in micelles than in adsorbed films and the repulsive interaction between DA^+ and the inorganic cation in the adsorbed film increased in the order $Na^+ < Ca^{2+} < La^{3+}$ [36].

The absence of copper ions at the interface implies that there exists negative adsorption. Negative adsorption is usually observed for inorganic salts and is caused by repulsive image forces between ions in the solution and electrostatic images in the air phase as well as an ion-free layer formed by the hydration of ions[37,38]. Also, Br^- has a stronger affinity toward the air-water interface than Cl^- and adsorbs preferentially[39].

The obtained experimental result supports this observation, i.e. although in bulk solution, concentration of Cl^- is twice higher than that of Br^-, but in the adsorbed film surface density of Br^- is about five times higher than that of Cl^-.

Combining the data obtained from all of the above techniques, it is possible to estimate the surface density of all the moieties present at the air water interface. The surface tension technique gives us the value of total surface excess concentration, Γ_{max} , 5.61 μ mol m^{-2} by eq. (1). Therefore, Γ_{max} or total surface excess concentration of ions can be written as:

$$\Gamma_{max} = \Gamma_{DTA} + \Gamma_{Cu} + \Gamma_{Br} + \Gamma_{Cl} = 5.61\ \mu\ \text{mol m}^{-2} \qquad (7)$$

Since, the electroneutrality condition holds for the total surface excess concentration of ions and for Γ_{max} as well we can write,

$$\Gamma_{DTA} + 2\,\Gamma_{Cu} = \Gamma_{Br} + \Gamma_{Cl} \qquad (8)$$

ERA-FTIR spectroscopy gives the concentration of dodecyltrimethyl ammonium chain to be Γ_{DTA} = 3.71 μ mol m^{-2} while Γ_{Br} determined using TRXAFS is 2.06 μ mol m^{-2}. Substituting these values in eqs. (7) and (8), Γ_{Cl} = 0.44 μ mol m^{-2} and Γ_{Cu} = -0.66 μ mol m^{-2} can be estimated. From this result, it is found that the adsorbed film is composed of mainly DTA^+, Br^- and Cl^-. Based on the above analysis the metallosurfactant orientation at the interface and in the bulk can be depicted as in Fig. 8 (a) and (b).

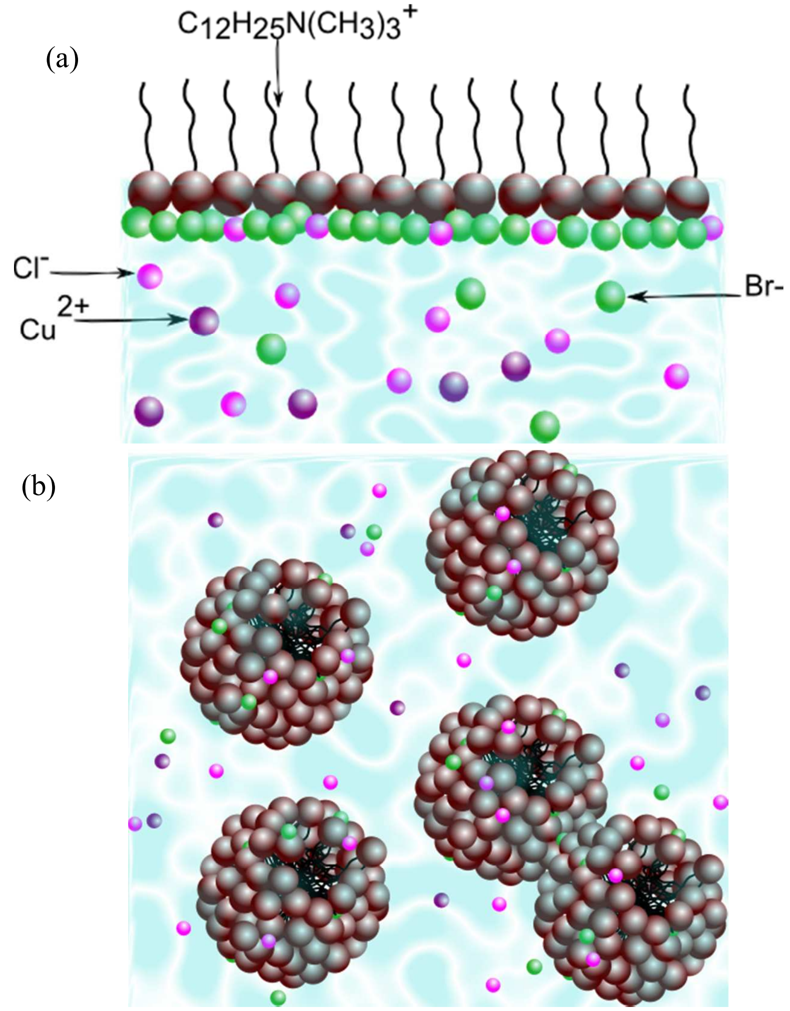

Fig. 8 Proposed organization of metallosurfactants, (a) at the air-water interface and (b) in the bulk aqueous solution.

4. Conclusions

The self aggregation behavior and molecular arrangement of the copper surfactant complex was completely analyzed with the aid of a number of complementary techniques. The copper surfactant complex shows a much lower cmc value than the reactant DTAB surfactant. A feasible situation for the adsorbed films of copper surfactant complex has been proposed. The results lead to some very interesting conclusions; (a) it could be fairly assumed that the copper metallosurfactant dissociates in aqueous solution where the surfactant ion, Cl^- and Br^- occupies the interface while the copper cation exists in the bulk solution, which is evident by the absence of copper ion peak in XAFS spectrum and negative surface density of copper at the air-water interface (b) copper cation acts just as an electrolyte added to the aqueous solution of surfactant DTAB which is corroborated by the lower cmc value and larger surface density (DTA) of copper surfactant complex compared to precursor cationic surfactant DTAB (c) geometry (curvature) of the surface of the aggregation influences the interaction between aggregates and metal ions. This has been inferred by TRXAFS experiments which reveal that Br^- ions exist in the bound-Br state at the interface and forms ion pairs. But, after micellization, in the bulk medium, Br^- ions may exist in either free or bound state. This indicates that degree of negative adsorption of copper ions (the interaction between the aggregates and metal ions) depends on the geometry of the surface of the aggregation. Therefore, a complete elucidation of the metallosurfactant organization at the air-water interface and in the bulk aqueous medium was carried out. Also, the surface densities and counter ion distribution were estimated. The results infer that copper does not exist in the inner core of micelles which implies that such system holds great potential for various catalytic applications.

Acknowledgments

SKM, RK and SG are thankful to Department of Science and Technology (DST) and Council of Scientific & Industrial Research (CSIR), India for the financial assistance and fellowship. The authors are thankful to DST-JSPS for the Bilateral Joint Research Project (DST/INT/JSPS/P-129/11). This work has been performed under the approval of the Photon Factory Advisory Committee (Proposal No. 2012 G518), which is greatly appreciated.

Notes and references

---

[1] M.J. Schick, Detergency in Nonionic Surfactants Physical chemistry, Marcel Dekker Inc. Press, New York, 1987, 758.

[2] D. Horter and J.B. Dressman, *Adv. Drug Deliv. Rev.*, 2001, **46**, 75-87.

[3] M. Mishra, P. Muthuprasanna, K.S. Prabha, P.S. Rani, I.A. Satishbabu, I.S. Chandiran and G. Arunachalam, *Int. J. Pharm. Tech. Res.*, 2009, **4**, 1354-1365.

[4] D.O. Shah, Surface Phenomenon in Enhanced Oil Recovery, Plenium Press, New York, 1981, 19.

[5] S. Saito, *J. Colloid Interface Sci.*, 1967, **24**, 227-234.

[6] F. Mancin, P. Scrimin, P. Tecilla and U. Tonellato, *Coord. Chem. Rev.*, 2009, **253**, 2150-2165.

[7] J. Zhang, X.G. Meng, X.C. Zeng, and X.Q. Yu, *Coord. Chem. Rev.*, 2009, **253**, 2166-2177.

[8] R. Kaur and S.K. Mehta, *Coord. Chem. Rev.,* 2014, **262**, 37-54.

[9] S. Paria and K.C. Khilar, *Adv. Colloid Interface Sci.*, 2004, **110**, 75-95.

[10] N.A. Negm and A.M. El Sabagh, *Quim. Nova*, 2011, **6**, 1007-1013.

[11] M.J. Rosen, Surfactants and Interfacial Phenomena, 2nd ed., John Wiley & Sons: New York, 1989, 122.

---

[12] K. Tamaki, *Colloid Polym. Sci.*, 1974, **252**, 547-550.

[13] S.C. Oh and D.O. Shah, *J. Phys. Chem.*, 1993, **97**, 284-286.

[14] J. Haldar, V.K. Aswal, P.S. Goyal and S. Bhattacharya, *J. Phys. Chem. B*, 2001, **105**, 12803-12808.

[15] D. Astruc, F. Lu and J.R. Aranzaes, *Angew. Chem. Int. Ed.*, 2005, **44**, 7852-7872.

[16] I.P. Beletskaya, A.N. Kashin, A.E. Litvinov, V.S. Tyurin, P.M. Valetsky and G. van Koten, *Organometallics*, 2006, **25**, 154-158.

[17] T. Yagyu, M. Tonami, K. Tsuchimoto, C. Takahashi and K. Jitsukawa, *Inorg. Chim. Acta*, 2012, **392**, 428–432.

[18] H.D. Jayathilake, J.A. Driscoll, A.N. Bordenyuk, L. Wu, S.R.P. da Rocha, C.N. Verani and A.V. Benderskii, *Langmuir*, 2009, **25**, 6880-6886.

[19] H. Nagatani, H. Tanida, I. Watanabe and T. Sagara, *Anal. Sci.*, 2009, **25**, 475-480.

[20] V.V. Kalinin and C.J. Radke, *Colloids Surf. A*, 1996, **114**, 337-350.

[21] I. Watanabe and H. Tanida, *Anal. Sci.*, 1995, **11**, 525-530.

[22] I. Watanabe, H. Tanida, S. Kawauchi, M. Harada and M. Nomura, *Rev. Sci. Instrum.*, 1997, **68**, 3307-3311.

[23] T. Takiue, Y. Kawagoe, S. Muroi, R. Murakami, N. Ikeda, M. Aratono, H. Tanida, H. Sakane, M. Harada and I. Watanabe, *Langmuir*, 2003, **19**, 10803-10807.

[24] M. Aratono, K. Kashimoto, T. Matsuda, S. Muroi, Y. Takata, N. Ikeda, T. Takiue, H. Tanida and I. Watanabe, *Langmuir,* 2005, **21**, 7398-7404.

[25] F. Hasanvand, R.A. Ahmadi and S. Amani, *Journal of Sciences, Islamic Republic of Iran*, 2012, **23**, 37-43.

[26] M. Aratono, M. Villeneuve, T. Takiue, N. Ikeda and H. Iyota, *J. Colloid and Interface Sci.*, 1998, **200**, 161-171.

[27] T. Takiue, Y. Kawagoe, S. Muroi, R. Murakami, N. Ikeda and M. Aratono, *Langmuir,* 2003, **19**, 10803-10807.

[28] K. Kashimoto, Y. Takata, T. Matsuda, N. Ikeda, H. Matsubara, T. Takiue, M. Aratono, H. Tanida and I. Watanabe, *Langmuir*, 2006, **22**,8403-8408.

[29] J. Mata, D. Varade and P. Bahadur, *Thermochim. Acta*, 2005, **428**,147-155.

[30] T. Yoshimura, A. Ohno and K. Esumi, *J. Colloid Interface Sci.*, 2004, **272**, 191-196.

[31] A.B. Mandal, B.U. Nair and D. Ramaswamy, *Langmuir*, 1988, **4**, 736-739.

[32] S. Azizian, K. Shibata, T. Matsuda, T. Takiue, H. Matsubara and M. Aratono, *J. Phys. Chem. B*, 2006, **110**, 17034-17042.

[33] K.M. Wilkinson, C.D. Bain, H. Matsubara and M. Aratono, *Chem. Phys. Chem.*, 2005, **6**, 547-555.

[34] I. Watanabe, H. Tanida, S. Kawauchi, and M. Harada, *Rev. Sci. Instrum.*, 1997, **68**, 3307-3311.

[35] Y. Imai, H.H. Li, H. Takumi, H. Tanida, I. Watanabe, T. Takiue, H. Matsubara and M. Aratono, *J. Colloid Interface Sci.*, 2012, **388**, 219-224.

[36] H. Iyota, T. Tomimitsu and M. Aratono, *J. Colloid Interface Sci.,* 2006, **302**, 330-334.

[37] C. Wagner, *Phys. Z*, 1924, **25**, 474.

[38] L. Onsager and N.N.T. Samaras, *J. Chem. Phys.*, 1934, **2**, 528-536.

---

[39] K. Kashimoto, K. Shibata, T. Matsuda, M. Hoshide and Y. Jimura, *Langmuir,* 2008, **24**, 6693-6697.

Table of Contents

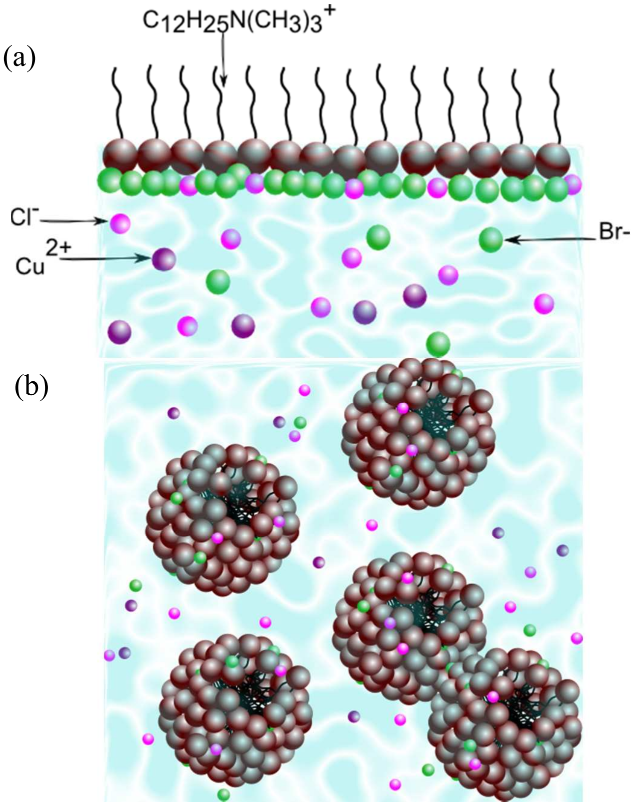

Aggregation behavior of metallosurfactant is pointing towards negative adsorption of metal ion at the micelle surface and surface adsorbed film